

Arecibo timing and single-pulse observations of 17 pulsars

D. J. Champion,^{1*} D. R. Lorimer,¹ M. A. McLaughlin,¹ K. M. Xilouris,²
Z. Arzoumanian,³ P. C. C. Freire,⁴ A. N. Lommen,⁵ J. M. Cordes⁶ and F. Camilo⁷

¹University of Manchester, Jodrell Bank Observatory, Macclesfield, Cheshire SK11 9DL

²University of Arizona, Steward Observatory, 933 N. Cherry Av. Bldg 65, Tucson, AZ 85721, USA

³USRA/EUD, NASA Goddard Space Flight Center, Code 662, Greenbelt, MD 20771, USA

⁴National Astronomy and Ionosphere Center, Arecibo Observatory, HC3 Box 53995, PR 00612, USA

⁵Department of Physics and Astronomy, Franklin and Marshall College, Box 3003, Lancaster, PA 17604, USA

⁶Department of Astronomy and Space Sciences, Cornell University, Ithaca, NY 14853, USA

⁷Columbia Astrophysics Laboratory, Columbia University, 550 West 120th Street, New York, NY 10027, USA

Accepted 2005 August 3. Received 2005 July 18; in original form 2005 May 20

ABSTRACT

We report on timing and single-pulse observations of 17 pulsars discovered at the Arecibo Observatory. The highlights of our sample are the recycled pulsars J1829+2456, J1944+0907 and the drifting subpulses observed in PSR J0815+0939. For the double neutron star binary J1829+2456, in addition to improving upon our existing measurement of relativistic periastron advance, we have now measured the pulsar's spin-period derivative. This new result sets an upper limit on the transverse speed of 120 km s^{-1} and a lower limit on the characteristic age of 12.4 Gyr. From our measurement of proper motion of the isolated 5.2-ms pulsar J1944+0907, we infer a transverse speed of $188 \pm 65 \text{ km s}^{-1}$. This is higher than that of any other isolated millisecond pulsar. An estimate of the speed, using interstellar scintillation, of $235 \pm 45 \text{ km s}^{-1}$ indicates that the scattering medium along the line of sight is non-uniform. We discuss the drifting subpulses detected from three pulsars in the sample, in particular the remarkable drifting subpulse properties of the 645-ms pulsar J0815+0939. Drifting is observed in all four components of the pulse profile, with the sense of drift varying among the different components. This unusual 'bi-drifting' behaviour challenges standard explanations of the drifting subpulse phenomenon.

Key words: radiation mechanisms: non-thermal – pulsars: general – pulsars: individual: PSR J0815+0939 – pulsars: individual: PSR J1829+2456 – pulsars: individual: PSR J1944+0907.

1 INTRODUCTION

Since the first systematic pulsar survey using the Arecibo Telescope (Hulse & Taylor 1974, 1975a,b) that discovered the original double neutron star binary B1913+16 (Hulse & Taylor 1975a), there have been a number of searches carried out with this sensitive system (e.g. Stokes et al. 1986; Nice, Fruchter & Taylor 1995). Timing of the pulsars discovered in these searches has provided a wealth of information, including the first evidence for the existence of gravitational radiation (Taylor & Weisberg 1982; Weisberg & Taylor 1984) and the first extrasolar planetary system (Wolszczan & Frail 1992).

Between 1994 and 1998 the telescope underwent a major upgradation, during which the receivers were parked on the meridian but observations could still be made as the sky drifted past. Pulsar

surveys conducted in this drift-scan mode have resulted in the discovery of 130 pulsars (Ray et al. 1995, 1996; Camilo et al. 1996; Lommen et al. 2000; McLaughlin et al. 2002; Lorimer et al. 2004, 2005).

In this paper, we report on timing and single-pulse observations of 17 pulsars discovered at Arecibo. Nine of the pulsars were discovered in our recent drift-scan searches (Champion et al. 2004; McLaughlin et al. 2004), while the remainder were found in earlier surveys and have not been subjected to a follow-up campaign of timing observations (Ray et al. 1996; Zepka et al. 1996; Nice 1999; McLaughlin, Cordes & Arzoumanian 2000). We discuss the timing results including the proper motion of millisecond pulsar (MSP) J1944+0907 and an updated timing solution for the relativistic binary J1829+2456. We then describe the drifting subpulses seen in three of the pulsars, including J0815+0939. This unique pulsar shows drifting in all four components of its unusual pulse profile, with the subpulses in one component drifting in a different sense to the others.

*E-mail: champion@jb.man.ac.uk

2 OBSERVATIONS AND ANALYSIS

The observations presented here were carried out between 1999 February and 2005 March using the Arecibo Telescope. Most of the observations used the 430-MHz Gregorian dome receiver, which has an average gain of 11 K Jy^{-1} and an average system temperature of 45 K, in combination with the Penn State Pulsar Machine (PSPM), a 128-channel analogue filterbank spectrometer (Cadwell 1997). During the early stages of timing when the periods of the pulsars were not well determined, the PSPM was used in search mode. The PSPM samples incoming voltages from the telescope every $80 \mu\text{s}$ over a bandwidth of 7.68 MHz. These data were then dedispersed by delaying successive channels in time corresponding to the nominal dispersion measure (DM) of each pulsar to produce time series that were subsequently folded to produce integrated pulse profiles. To confirm that the period was the fundamental rather than a harmonic, the data were folded at twice the period and the profile was checked. Once the period of each pulsar had been determined accurately, the timing mode of the PSPM was used. In timing mode, the data in each frequency channel were folded online. The 128 individual profiles can then be dedispersed and summed to produce a single profile.

The first stage of timing analysis is to produce a high signal-to-noise ratio (S/N) profile to use as a template. Initially, this was done by shifting the profile so the peak was at a phase of 0.5 before summing the profiles. The time of arrival (TOA) of each profile was then calculated by convolving the profile with the template and adding this offset to the start time of the observation. These TOAs were then analysed with the TEMPO software package¹ to produce a preliminary phase-connected solution (where every rotation of the pulsar is accounted for) over the time-span of the observations. In most cases a simple spin-down model with five free parameters [pulse phase, period, period derivative, right ascension (RA) and declination (Dec.)] was used. For PSR J1944+0907 the proper motion is a significant effect and is included in the fit. The relativistic binary pulsar J1829+2456 requires an additional five classical and two relativistic parameters to produce a phase-connected solution. For each pulsar the resulting ephemeris was used to predict the pulse phase of each profile. These were then aligned before they were summed to produce a better template that was subsequently used to generate new TOAs, weighted by S/N, which were analysed using TEMPO. This additional iteration often resulted in significant reduction of the root mean square (rms) observed minus model timing residual. With the exception of PSR J1917+0834, a single template was sufficient for the timing analysis. For J1917+0834, due to the short length of the integrations and long period of the pulsar, only a small number of pulses were summed causing the relative strengths of the two peaks in the profile to vary from observation to observation, a template for each mode was required to provide accurate TOAs in the initial stages.

Most of the previously published DM measurements were based on the original observations and so were poorly constrained. In 2004 December the pulsars were observed at 320, 327, 334 and 430 MHz using the PSPM. The TOAs produced were analysed using TEMPO by holding all the (now well-constrained) parameters of the ephemeris constant and fitting for DM. This new value of DM was then used to dedisperse the data again and improve the template, TOAs and ultimately the ephemerides.

To calibrate the intensity scale of the pulse profiles, we followed the procedure described by Lorimer, Camilo & Xilouris (2002) and

scaled each profile by the factor of $1000T/(DG) \text{ mJy}$, where T is the total system noise temperature (K), D is the DC offset of the profile (in PSPM counts) and G is the antenna gain (K Jy^{-1}). Due to the design of the Arecibo Telescope, both T and G are strong functions of zenith angle. This dependence is described analytically by Perillat (1999). The total system temperature also includes the background sky temperature contribution (Haslam et al. 1982). The error is based on the standard deviation (s.d.) of the observed fluxes.

3 TIMING RESULTS

The basic timing parameters, pulse widths and flux densities are summarized in Table 1. Listed are the pulsar name, position (in RA and Dec.), period P , its derivative \dot{P} and epoch, DM, span of observations, number of TOAs and the post-fit weighted rms of the timing residuals. Table 2 lists the additional timing parameters for the binary pulsar J1829+2456 and the isolated MSP J1944+0907. The 430-MHz profiles derived from a phase-coherent sum over many individual observations are shown in Fig. 1.

Further observed and derived parameters are summarized in Table 3. Listed are the pulse widths at 10 per cent, w_{10} , and 50 per cent, w_{50} , of peak amplitude; the equivalent pulse width (the width of a top hat function with the same integrated flux and peak amplitude), w_{eq} ; the mean 430-MHz phase-averaged flux density, S_{430} ; the distance d [inferred from the free-electron density model of Cordes & Lazio (2002)]; Galactic height ($z = d \sin b$, where b is the Galactic latitude); 430-MHz luminosity ($L_{430} \equiv S_{430}d^2$); spin-down age ($\tau = P/2\dot{P}$); spin-down energy-loss rate ($\dot{E} = 4\pi^2 I \dot{P}/P^3$, where the neutron star moment of inertia I is taken to be 10^{45} g cm^2); and inferred surface dipole magnetic field strength ($B = 3.2 \times 10^{19} \sqrt{P\dot{P}} \text{ G}$, Lorimer & Kramer 2005).

In Fig. 2, we show the locations of the 17 pulsars on the period–period derivative ($P-\dot{P}$) diagram. As can be seen, the majority of the pulsars occupy the lower end of the ‘island’ of points suggesting that they are relatively old members of the normal population. This is in keeping with previous samples of pulsars drawn from low-frequency surveys (e.g. Lorimer et al. 2002) that are less effective at finding young pulsars than surveys at higher frequencies (e.g. Manchester et al. 2001).

3.1 PSR J1829+2456

This 41-ms pulsar is in a mildly eccentric binary system where the companion is most likely a neutron star (Champion et al. 2004). The rate of advance of periastron, $\dot{\omega}$, is now measured to a significance of 180σ . Interpreting $\dot{\omega}$ as purely relativistic precession implies that the total mass of the binary $M = 2.59 \pm 0.02 M_{\odot}$ (see Fig. 3). The lower companion mass limit of $1.26 M_{\odot}$, and upper limit to the pulsar mass of $1.34 M_{\odot}$ are given by the constraint that the inclination angle $i \leq 90^\circ$. A very conservative upper limit on the companion mass $M_c = 2.61 M_{\odot}$, and a minimum inclination angle $i > 29^\circ$, can also be inferred. A more likely upper limit of $M_c = 1.33 M_{\odot}$ is obtained by assuming a minimum pulsar mass of $1.26 M_{\odot}$ (the lowest measured mass of any neutron star, namely PSR J0737–3039B, Lyne et al. 2004). An upper limit of 8 ms can now also be placed on the relativistic time-dilation and gravitational redshift parameter, γ , but, as shown in Fig. 3, this is not yet constraining. The determination of these limits is described in more detail in Champion et al. (2004).

The extended baseline of our TOAs has also resulted in a measurement of \dot{P} for this pulsar. However, this \dot{P} should be treated with

¹ <http://pulsar.princeton.edu/tempo>.

Table 1. Observed parameters of the 17 pulsars derived from the TEMPO timing analysis described in Section 2. Figures in parentheses are 1σ uncertainties in the least significant digits. The arrival times from which these ephemerides are derived are freely available online as part of the European Pulsar Network (EPN) data base (<http://www.jb.man.ac.uk/~pulsar/Resources/epn>).

Name (PSR)	RA (J2000) (h:m:s)	Dec. (J2000) ($^{\circ}$: ' : ")	P (s)	\dot{P} (10^{-15})	Epoch (MJD) ^a	DM (pc cm^{-3})	Span (MJD) ^a	N_{TOAs}	rms (μs)
J0152+0948	01:52:23.73 (5)	+09:48:10 (2)	2.746 647 290 14 (10)	1.700 (4)	528 58	21.87 (2)	525 97–530 04	26	350
J0546+2441	05:46:28.76 (3)	+24:41:21 (6)	2.843 850 385 24 (6)	7.65 (3)	529 14	73.81 (3)	527 07–531 19	29	706
J0815+0939	08:15:08.776 (9)	+09:39:50.7 (6)	0.645 161 191 06 (5)	0.139 (6)	528 54	52.667 (9)	526 00–527 96	53	270
J1503+2111	15:03:54.60 (4)	+21:11:09.3 (5)	3.314 001 501 22 (12)	0.14 (2)	528 57	11.75 (6)	525 95–531 18	12	941
J1746+2245	17:46:00.84 (3)	+22:45:28.9 (8)	3.465 037 782 64 (6)	4.919 (7)	527 65	52.0 (20)	524 01–531 29	19	1240
J1807+0756	18:07:51.235 (2)	+07:56:43.39 (5)	0.464 300 493 199 (2)	0.1294 (2)	530 64	89.29 (3)	527 65–533 62	22	134
J1821+1715	18:21:13.503 (4)	+17:15:47.06 (7)	1.366 682 059 422 (10)	0.8714 (11)	530 64	60.47 (7)	527 65–533 62	23	240
J1829+2456	18:29:34.6668 (2)	+24:56:18.193 (3)	0.041 009 823 581 17 (4)	0.000 0525 (15)	528 87	13.8 (5)	527 85–534 47	50	22
J1843+2024	18:43:26.18 (7)	+20:24:54.6 (12)	3.406 538 6707 (4)	1.04 (4)	530 64	85.3 (2)	527 65–533 62	19	3829
J1849+2423	18:49:34.6763 (4)	+24:23:45.976 (12)	0.275 641 498 671 01 (7)	0.152 582 (4)	521 99	62.239 (5)	511 94–529 23	244	409
J1915+0752	19:15:01.94 (2)	+07:52:09.2 (6)	2.058 313 788 61 (7)	0.139 (9)	530 48	105.3 (3)	527 33–533 62	60	2891
J1916+0748	19:16:51.5 (2)	+07:48:00 (5)	0.541 752 113 81 (17)	10.708 (17)	530 48	304.0 (15)	527 33–533 62	15	14754
J1917+0834	19:17:48.853 (6)	+08:34:54.63 (14)	2.129 665 364 024 (4)	17.4935 (2)	523 45	29.18 (6)	513 27–533 62	36	608
J1933+0758	19:33:19.407 (2)	+07:58:07.01 (7)	0.437 454 407 217 (2)	0.2183 (2)	530 48	165.02 (4)	527 32–533 62	19	171
J1944+0907	19:44:09.32084 (3)	+09:07:23.2388 (12)	0.005 185 201 904 1260 (3)	0.000 017 13 (2)	529 13	24.34 (2)	527 32–534 47	27	2.6
J2007+0910	20:07:58.1031 (12)	+09:10:12.93 (6)	0.458 734 825 8074 (6)	0.332 44 (12)	529 94	48.6 (2)	525 95–533 92	25	116
J2045+0912	20:45:47.3438 (9)	+09:12:29.16 (4)	0.395 555 111 7394 (5)	0.195 20 (7)	529 97	31.776 (4)	526 01–533 92	25	78

^aModified Julian Date.

Table 2. Additional parameters for pulsars J1829+2456 and J1944+0907. Figures in parentheses are 1σ uncertainties in the least significant digits.

Name (PSR)		
J1829+2456	x , projected semimajor axis (lt-sec)	7.238 (2)
	P_b , binary period (d)	1.176 027 941 (16)
	e , eccentricity	0.139 1412 (19)
	ω , longitude of periastron (deg)	229.92 (2)
	T_0 , epoch of periastron (MJD)	528 48.579 775 (3)
	$\dot{\omega}$, rate of advance of periastron (deg yr^{-1})	0.2919 (16)
	γ , relativistic time-dilation and gravitational redshift (ms)	3.6 (38)
	Mean TOA uncertainty (μs)	33.7
J1944+0907	μ_α , proper motion in RA (mas yr^{-1})	12.0 (7)
	μ_δ , proper motion in Dec. (mas yr^{-1})	−18 (3)
	Mean TOA uncertainty (μs)	3.6

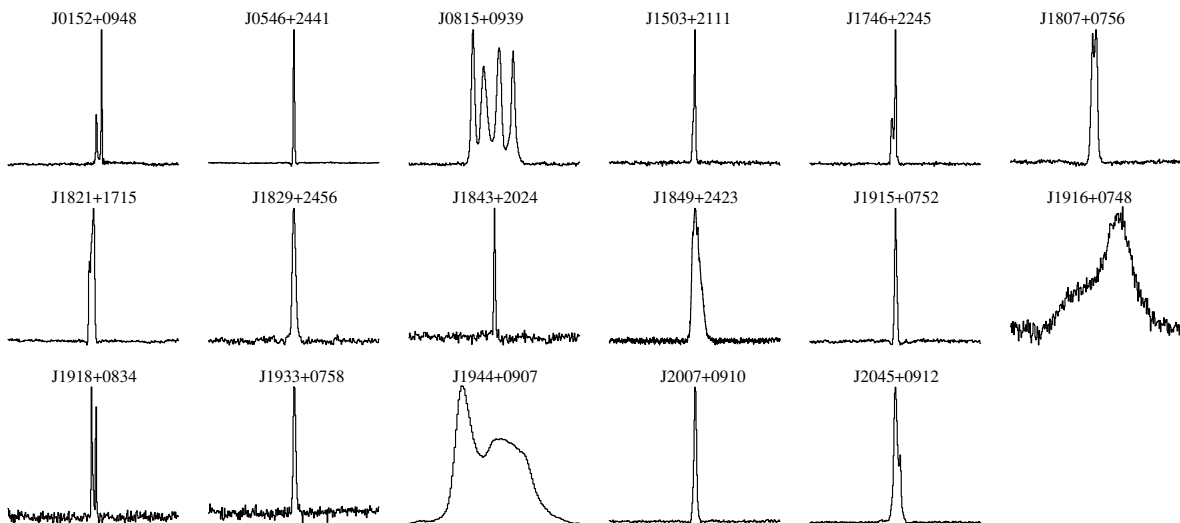


Figure 1. Integrated 430-MHz pulse profiles. All profiles show full-pulse phase over 256 bins with the exception of PSR J1944+0907 that has 128 bins. PSR J1944+0907 is dispersion-smearred over ~ 4 bins. These profiles are freely available as part of the European Pulsar Network (EPN) data base.

Table 3. Pulse profile widths, 430-MHz flux-density measurements and various derived parameters for the 17 pulsars. All distance measurements have statistical error of 25 per cent as estimated by Cordes & Lazio (2002); individual errors may be larger. Figures in parentheses are 1σ uncertainties in the least significant digits for the observed parameters. For PSR J1944+0907, the Shklovskii-corrected \dot{P} has been used to calculate the luminosity, spin-down age, spin-down energy-loss rate and inferred surface dipole magnetic field strength.

Name (PSR)	w_{10} (ms)	w_{50} (ms)	w_{eq} (ms)	S_{430} (mJy)	d (kpc)	z (kpc)	L_{430} (mJy kpc ²)	Log τ (kyr)	Log \dot{E} (erg s ⁻¹)	Log B (G)
J0152+0948	103	11	17	0.91(3)	0.9	-0.71	0.7	4.4	30.5	12.3
J0546+2441	51	28	25	2.65(10)	2.0	-0.07	10.6	3.8	31.1	12.7
J0815+0939	183	166	75	3.7(2)	2.5	0.98	23.1	4.9	31.3	11.5
J1503+2111	80	26	39	1.3(2)	1.0	0.88	1.3	5.6	29.2	11.8
J1746+2245	125	34	50	1.26(7)	3.0	1.22	10.8	4.1	30.7	12.6
J1807+0756	27.3	18.2	17.6	2.16(6)	3.5	0.81	26.5	4.8	31.7	11.4
J1821+1715	64	45	39	3.7(2)	2.8	0.70	29.0	4.4	31.1	12.0
J1829+2456	1.7	0.8	1.0	0.3(1)	1.2	0.33	0.4	7.1	31.5	9.2
J1843+2024	29	40	29	0.37(3)	4.0	0.75	5.9	4.7	30.0	12.3
J1849+2423	26.1	14.4	14.6	2.3(6)	3.2	0.63	23.6	4.5	32.5	11.3
J1915+0752	60	24	28	1.70(10)	3.8	-0.11	24.6	5.4	29.8	11.7
J1916+0748	230	80	50	1.14(9)	8.1	-0.29	74.8	2.9	33.4	12.4
J1917+0834	81	68	35	0.44(10)	1.9	-0.06	1.6	3.3	31.9	12.8
J1933+0758	14.6	6.8	6.8	0.34(3)	6.0	-0.58	12.2	4.5	32.0	11.5
J1944+0907	2.5	0.5	0.5	3.9(3)	1.8	-0.23	12.6	7.1	33.2	8.3
J2007+0910	16.6	8.3	8.7	1.51(5)	2.0	-0.55	6.0	4.3	32.1	11.6
J2045+0912	25.5	10.4	13.7	3.5(2)	1.9	-0.66	12.6	4.5	32.1	11.5

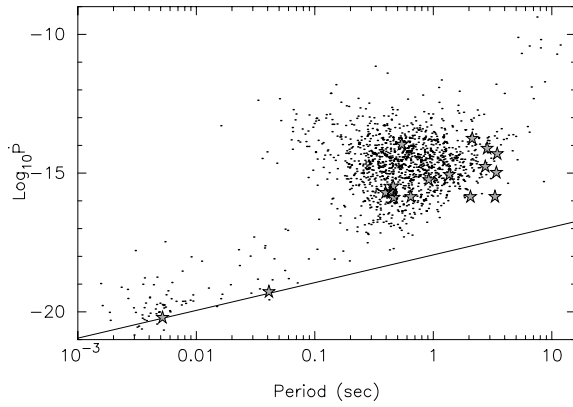


Figure 2. The P - \dot{P} diagram showing all currently known pulsars listed in the online Australia Telescope National Facility (ATNF) pulsar catalogue (<http://www.atnf.csiro.au/research/pulsar/psrcat>). The stars indicate the 17 pulsars in the current sample. Young pulsars are in the top right-hand side of the plot while old recycled pulsars are in the bottom left-hand side. The line indicates the age of the Universe, $\tau = 14$ Gyr, equivalent to $H_0 = 70 \text{ km s}^{-1} \text{ Mpc}^{-1}$ (York et al. 2005). The \dot{P} of PSR J1944+0907 has been Shklovskii-corrected assuming the DM-inferred distance (see Section 3.2). The \dot{P} of PSR J1829+2456, for which there currently exists no proper motion measurement, has not been Shklovskii-corrected (see Section 3.1).

caution since any transverse component of proper motion of the system would lead to secular acceleration (Shklovskii 1970; Camilo, Thorsett & Kulkarni 1994) and will contribute to the observed period derivative,

$$\frac{\dot{P}}{P} = \frac{1}{c} \frac{V_T^2}{d} = 2.43 \times 10^{-21} \text{ s}^{-1} \left(\frac{d}{\text{kpc}} \right) \left(\frac{\mu_T}{\text{mas yr}^{-1}} \right)^2, \quad (1)$$

where \dot{P} is contribution due to the proper motion, V_T is the transverse speed and μ_T is the proper motion. Indeed, assuming the current measurement of \dot{P} is entirely due to proper motion, and adopting the nominal DM-derived distance of 1.2 kpc, the Shklovskii-effect

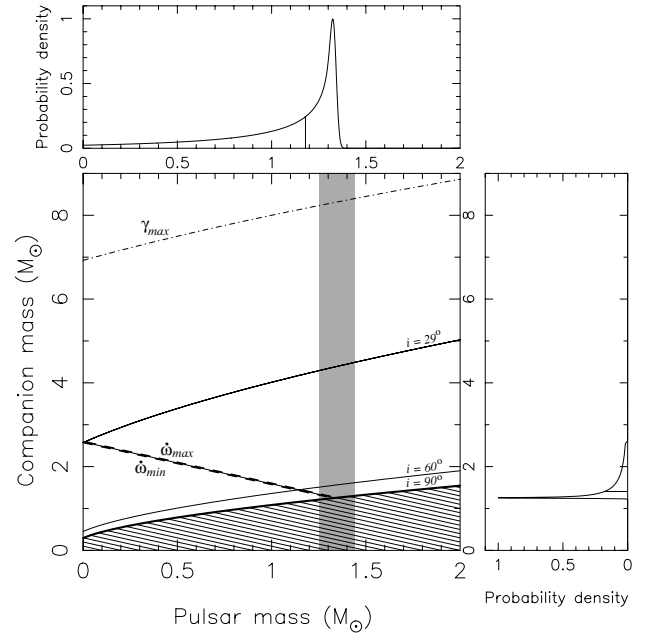


Figure 3. Current constraints on the masses of PSR J1829+2456 and companion. The grey bar shows the mass limits for neutron stars, the upper limit described by Thorsett & Chakrabarty (1999) and the low measured mass of PSR J0737-3039B (Lyne et al. 2004). There is currently only an upper limit for the time-dilation and redshift parameter, γ . The upper and lower limits of $\dot{\omega}$ are now so close that they appear as one thick line. The masses of the system are constrained to be between the two $\dot{\omega}$ limits and above the $i = 90^\circ$ limit. The marginal figures show the probability density functions for the pulsar and companion masses assuming a random distribution of inclination angles. The lines of constant mass indicate the median of the distributions.

places an upper limit of 20 mas yr^{-1} on the proper motion, corresponding to a transverse speed of $\sim 118 \text{ km s}^{-1}$. This transverse speed is consistent with other double neutron star systems so it is possible that the intrinsic \dot{P} is considerably lower.

However if the \dot{P} of PSR J1829+2456 is assumed to be intrinsic, it places this double neutron star system in an area of the $P-\dot{P}$ diagram inhabited by various eccentric binary systems (see Fig. 2). This \dot{P} implies a characteristic age of at least 12.4 Gyr and a magnetic field strength of 1.5×10^9 G. As for other recycled pulsars this large characteristic age suggests that its birth spin period was comparable to its current spin period. Of the other double neutron star systems, only J1518+4904 has a lower \dot{P} (Hobbs et al. 2004b). PSR J1829+2456 is currently the subject of an extended timing campaign to measure a proper motion and so remove any contribution of the Shklovskii-effect from the measurement of \dot{P} . Simulated TOAs suggest that a proper motion of 15 mas yr^{-1} should be measured to ~ 30 per cent and the expected γ (1.3 ms) should be measured to ~ 40 per cent accuracy within the next year. Simulations also suggest that it would be possible to measure the Shapiro-delay with the current observing equipment if the inclination was $\sim 90^\circ$.

3.2 PSR J1944+0907

PSR J1944+0907 is an isolated 5.2-ms pulsar with a broad profile (McLaughlin et al. 2005). Isolated MSPs are rare objects; only 13 are currently known (Lorimer 2005). While binary MSPs are thought to be spun-up by the accretion of matter from an evolved binary companion, the formation process for isolated MSPs is presently not clear. Either they form through a different formation channel (such as accretion-induced collapse), or they ablate their companion with their strong relativistic wind (Ruderman, Shaham & Tavani 1989). As shown in Fig. 4, the proper motion of this pulsar, μ_T , is detected very significantly in our timing observations from which we obtain $\mu_T = 22 \pm 2 \text{ mas yr}^{-1}$. This would imply a transverse speed $V_T = \mu_T d = 188 \pm 65 \text{ km s}^{-1}$; this is significantly higher than the average for recycled systems (87 ± 13 , Hobbs et al. 2005) and, with the exception of PSR B1257+12 that has a planetary system, this is by far the highest of all isolated (and indeed most binary) MSPs so far (Camilo, Nice & Taylor 1993, 1996; Cognard et al. 1995; Nice & Taylor 1995; Toscano et al. 1999; Lommen et al. 2000; Wolszczan et al. 2000; Edwards & Bailes 2001; Faulkner et al. 2004; Hobbs et al. 2004a; Lorimer et al. 2004).

The very large transverse speed implied by the proper motion would have a significant effect on the observed \dot{P} as described in Section 3.1. When this Shklovskii-effect is taken into account the intrinsic \dot{P} drops to 6.2×10^{-21} . This value has been used to calculate the derived parameters listed in Table 3.

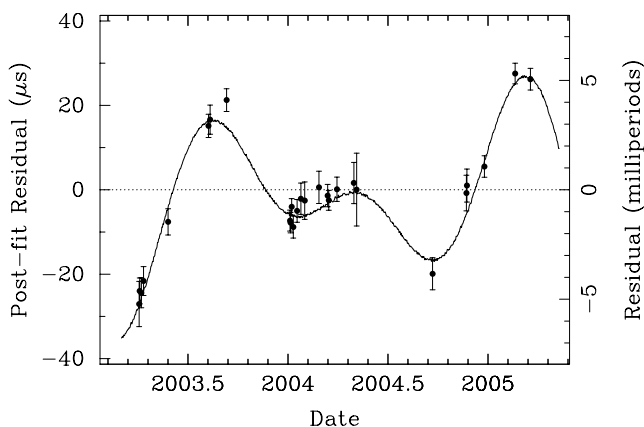


Figure 4. The timing residuals for PSR J1944+0907 before fitting for proper motion. The solid line indicates the fit for a proper motion of 22 mas yr^{-1} .

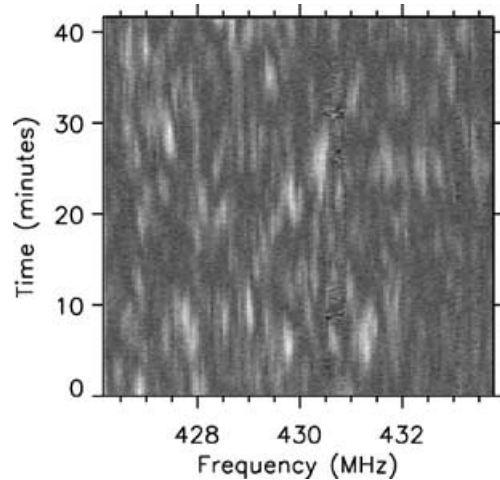


Figure 5. Dynamic spectrum (i.e. onpulse intensity versus time and frequency) for J1944+0907 at 430 MHz. The intensity is indicated by the linear grey-scale (black: low intensity, white: high intensity). The spectrum was formed with 10-s integrations using the PSPM, with 128 frequency channels across the 7.68-MHz bandwidth.

PSR J1944+0907 also scintillates strongly at 430 MHz, as shown in Fig. 5. An auto-correlation analysis of its dynamic spectrum indicates a bandwidth and time-scale of $\Delta\nu_d = 90 \text{ kHz}$ and $\Delta t_d = 101 \text{ s}$. The interstellar scintillation-derived transverse speed, V_{ISS} , is given by

$$V_{\text{ISS}} = \frac{A d^{1/2} \Delta\nu_d^{1/2}}{\nu \Delta t_d}, \quad (2)$$

where the constant $A = 2.53 \times 10^4 \text{ km s}^{-1}$ for a uniform Kolmogorov scattering medium, d is the distance (kpc), ν is frequency (GHz), $\Delta\nu_d$ is the scintillation bandwidth (MHz) and Δt_d is the scintillation time-scale (s) (Cordes & Rickett 1998). Assuming a distance of $1.8 \pm 0.5 \text{ kpc}$, the implied transverse speed is $235 \pm 45 \text{ km s}^{-1}$.

Because the transverse speeds inferred from proper motion and scintillation depend differently on the distance, we may use these measurements to calculate a distance consistent with both measurements. Assuming a uniform scattering medium, this distance is 3.6 kpc, with implied transverse speed of 340 km s^{-1} . Not only is this far higher than the transverse speeds measured for any isolated MSPs but would imply a Shklovskii-correction greater than the observed \dot{P} . We therefore conclude that the scattering medium is not uniform and that the actual distance and speed are closer to 1.8 kpc and 188 km s^{-1} , respectively.

4 DRIFTING SUBPULSE BEHAVIOUR

Single pulses often consist of several components, called subpulses, which change position, often drifting from pulse to pulse. This phenomenon was first reported by Drake & Craft (1968) and has since been recognized in roughly 100 radio pulsars (Weltevrede, Edwards & Stappers 2000). It is usually understood within the $\mathbf{E} \times \mathbf{B}$ drift model of Ruderman & Sutherland (1975) in which radio emission comes from discrete locations, or ‘subbeams’, positioned on a circle around the magnetic pole. The subbeams rotate and move in and out of our line of sight. The Ruderman–Sutherland model has been fairly successful in explaining pulsar drifting patterns. In fact, for PSR B0943+10, Deshpande & Rankin (1999) have been able to

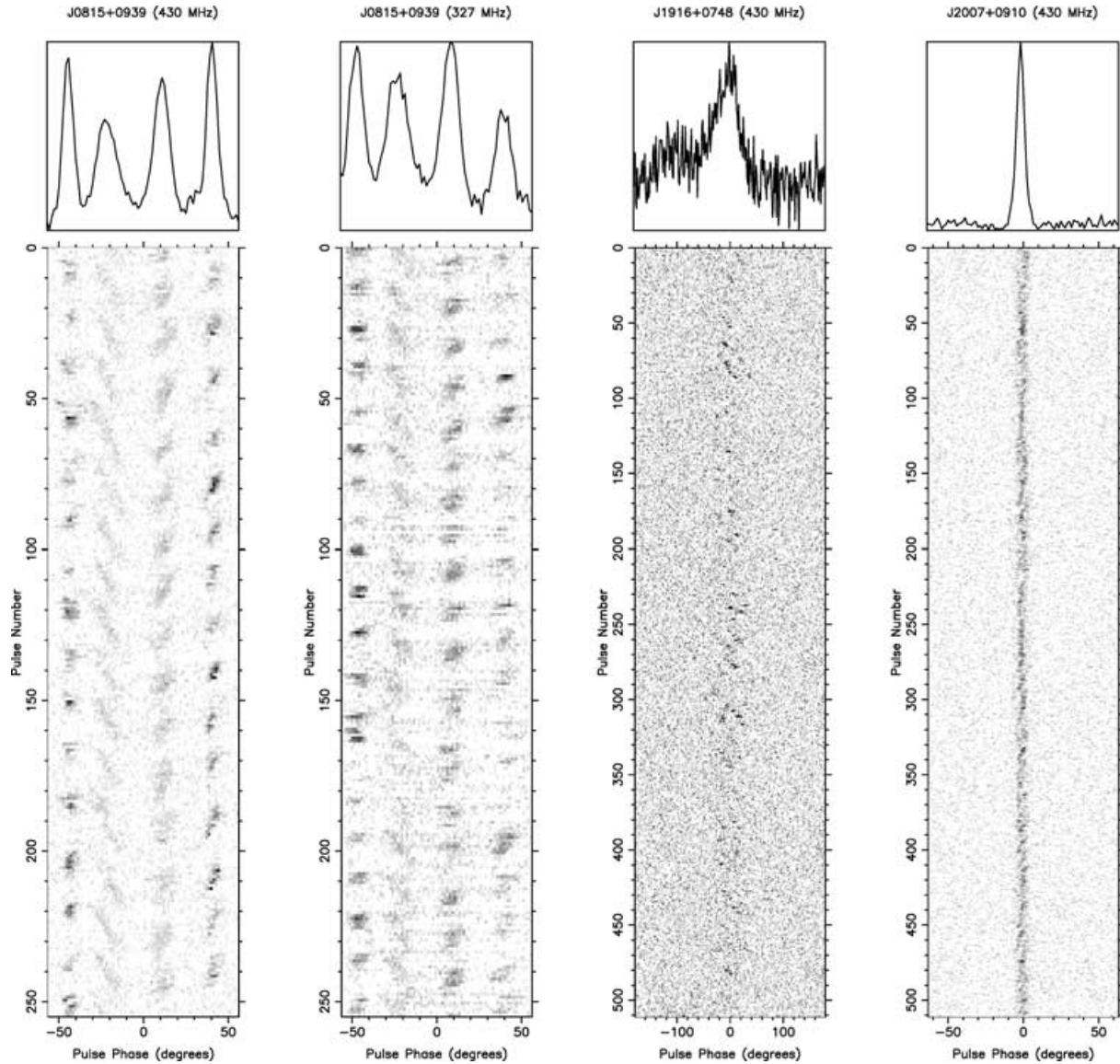


Figure 6. The single pulses for pulsars J0815+0939, J1916+0748 and J2007+0912. The intensity is indicated by the linear grey-scale (white: low intensity, black: high intensity). The drifting can be seen as diagonal stripes. In PSR J0815+0939, it is clear that the second component drifts in the opposite sense to the third and fourth. Drifting in the first component is unclear and seems to show some sense reversal.

determine that there are 20 subbeams rotating around this pulsar’s magnetic axis, with a rotation time-scale close to 100 s.

In some cases, our PSPM search-mode data were of sufficiently high quality to analyse individual pulses. In our sample, three of the pulsars show drifting subpulses. The drifting can be characterized by the drift rate and two periods (P_2 and P_3 , Backer 1973). The drift rate is simply the longitude of pulse phase drifted by each subpulse per second. The separation in longitude between consecutive subpulses and the separation at a given longitude between successive subpulses are denoted by P_2 and P_3 , respectively. The single pulses for the three pulsars are shown in Fig. 6 and the measured drift rate and P_3 for each pulsar are listed in Table 4; P_2 is not applicable in these cases as there is never more than one subpulse (per component) visible during a single pulse. For PSR J0815+0939, P_3 was determined using a fluctuation spectrum analysis, in which a Fourier transform is applied to a series of single pulses (in this case 256) for a range of pulse longitudes.

The single-pulse behaviour of the 645-ms pulsar J0815+0939 is remarkable. This pulsar’s profile is unusual, consisting of four components with separations of 41, 58 and 54 ms and not easily described by standard phenomenological classification schemes (Rankin 1983). As shown in Fig. 6, drifting is observed within all four components. We refer to these (from left to right) as components I, II, III and IV. The drift within component I is difficult to measure and appears to change sense within an observation. The drift rates of components II, III and IV are very stable from epoch to epoch and do not appear to change sense. However, the drift sense of component II differs from those of components III and IV. While of opposite sign, the drift rates of components II and IV are equal within the errors, indicating a possible relationship. Measurements at 327 and 430 MHz indicate an evolution of the drift rate with frequency, with a higher drift rate at the lower frequency.

While drift sense reversals within a single component are quite common and are attributed to aliasing effects (Gupta et al. 2004),

Table 4. Parameters obtained from our analyses of the single-pulse observations described in Section 4. Figures in parentheses are 1σ uncertainties in the least significant digits. These parameters are derived from the highest S/N observation for each pulsar, but the drifting properties appear to be consistent from epoch to epoch. A more detailed study of the time-evolution of the drifting properties of J0815+0939 will be presented elsewhere.

Name (PSR)	Frequency (MHz)	Component	Drift rate (deg s ⁻¹)	P_3 (s)
J0815+0939	430	I	-	10.87 (16) ^a
		II	-1.60 (13)	10.87 (16) ^a
		III	2.46 (19)	10.87 (16) ^a
		IV	1.57 (16)	10.87 (16) ^a
	327	I	-	8.72 (16) ^a
		II	-2.3 (5)	8.72 (16) ^a
		III	3.2 (8)	8.72 (16) ^a
		IV	2.68 (18)	8.72 (16) ^a
J1916+0748	430	I	5.4 (14)	8.6 (8)
J2007+0912	430	I	1.7 (6)	5.4 (7)

^aDetermined from fluctuation spectra. Uncertainties are determined by the resolution of the spectra.

it is rare for different components to show different drift senses (Hankins & Wolszczan 1987; Weltevrede et al. 2005). How do we interpret this strange behaviour? It is very difficult to reconcile with the standard Ruderman–Sutherland model in which sparks travel around a circular region centred on the pulsar’s magnetic axis. In this case, the four components would probably be associated with two nested hollow-cone beams. Similar drift sense would be expected in components I and IV and also II and III but this is not observed. This pulsar’s ‘bi-drifting’ behaviour has been geometrically modelled by Qiao et al. (2004). While promising, this model is based on one short integration at one frequency. Edwards & Stappers interpret the behaviour of B1918 + 19 as being due to multiple imaging of sub-beam systems. Further studies are planned that will determine if there are any aliasing effects while polarization measurements will help determining the relationship between the multiple components.

In addition to J0815+0939, both PSR J1916+0748 and J2007+0912 show weak drifting as shown in Fig. 6. For J1916+0748, the broad integrated profile can be explained as the superposition of a series of drifting subpulses. Further studies of these pulsars with higher sensitivity and time-resolution in future may well be worthwhile.

5 CONCLUSIONS

We have presented a timing and single-pulse study of a sample of 17 pulsars discovered with the Arecibo Telescope. These observations provide new insights into a wide range of neutron star physics. We now briefly summarize the new results obtained from the present study.

Extending the timing baseline of the relativistic binary pulsar J1829+2456 presented by Champion et al. (2004) has allowed the mass of the system to be further constrained, $M = 2.59 \pm 0.02 M_{\odot}$, and an upper limit to be placed on the relativistic time-dilation and gravitational redshift parameter, $\gamma < 8$ ms. The measurement of $\dot{P} = (5.25 \pm 0.15) \times 10^{-20}$ has placed an upper limit on the proper motion, $\mu_T = 20$ mas yr⁻¹, (using the Shklovskii-effect) and a lower limit on the characteristic age, $\tau \sim 12.4$ Gyr. Further timing will allow a measurement of this pulsar’s proper motion and a determination of the intrinsic \dot{P} . A measurement of the parallax through timing is less likely as the current level of precision.

The proper motion of PSR J1944+0939 has been measured and revealed the highest transverse speed of any isolated MSP, $V_T = 188 \pm 65$ km s⁻¹. An alternative estimate of the speed using interstellar scintillation, $V_{ISS} = 235 \pm 45$ km s⁻¹, demonstrates that

the scattering medium along the line of sight is non-uniform. These measurements suggest that the space velocity of J1944+0939 is higher than for any other isolated MSP. Further timing observations will ultimately allow the parallax of this pulsar to be measured, which will resolve current uncertainties in the transverse speed estimates.

The drifting observed in PSR 0815+0939 is very unusual and warrants further study. All four components of the pulse profile show drifting subpulse behaviour. Of the three components in which we see no drift sense reversals, one of the components has a different drift sense to the others. This is difficult to explain using the standard Ruderman–Sutherland model. Further observations, including polarimetry, are required to shed light on this remarkable pulsar and the implications it may have for emission mechanism models.

ACKNOWLEDGMENTS

The Arecibo Observatory, a facility of the National Astronomy and Ionosphere Center, is operated by Cornell University in a co-operative agreement with the National Science Foundation (NSF). We thank Alex Wolszczan for making the PSPM freely available for use at Arecibo. Without this superb instrument, the results presented here would not have been possible. DJC is funded by the Particle Physics and Astrophysics Research Council. DRL is a University Research Fellow funded by the Royal Society. ZA is supported by NASA grant NRA-99-01-LTSA-070. FC is supported by the NSF and NASA.

REFERENCES

- Backer D. C., 1973, ApJ, 182, 245
- Cadwell B. J., 1997, PhD thesis, Penn State Univ.
- Camilo F., Nice D. J., Shrauner J. A., Taylor J. H., 1996, ApJ, 469, 819
- Camilo F., Nice D. J., Taylor J. H., 1993, ApJ, 412, L37
- Camilo F., Nice D. J., Taylor J. H., 1996, ApJ, 461, 812
- Camilo F., Thorsett S. E., Kulkarni S. R., 1994, ApJ, 421, L15
- Champion D. J., Lorimer D. R., McLaughlin M. A., Arzoumanian Z. A., Cordes J. M., Weisberg J., Taylor J. H., 2004, MNRAS, 350, L61
- Cognard I., Bourgois G., Lestrade J. F., Biraud F., Aubry D., Darchy B., Drouhin J. P., 1995, A&A, 296, 169
- Cordes J. M., Lazio T. J. W., 2002, NE2001.I. A New Model for the Galactic Distribution of Free Electrons and its Fluctuations, preprint (astro-ph/0207156)
- Cordes J. M., Rickett B. J., 1998, ApJ, 507, 846
- Deshpande A. A., Rankin J. M., 1999, ApJ, 524, 1008

- Drake F. D., Craft H. D., 1968, *Nat*, 220, 231
 Edwards R. T., Bailes M., 2001, *ApJ*, 547, L37
 Edwards R. T., Stappers B. W., 2003, *A&A*, 407, 273
 Faulkner A. J. et al., 2004, *MNRAS*, 355, 147
 Gupta Y., Gil J., Kijak J., Sendyk M., 2004, *A&A*, 426, 229
 Hankins T. H., Wolszczan A., 1987, *ApJ*, 318, 40
 Haslam C. G. T., Stoffel H., Salter C. J., Wilson W. E., 1982, *A&AS*, 47, 1
 Hobbs G. et al., 2004a, *MNRAS*, 352, 1439
 Hobbs G., Lyne A. G., Kramer M., Martin C. E., Jordan C., 2004b, *MNRAS*, 353, 1311
 Hobbs G., Lormier D. R., Lyne A. G., Kramer M., 2005, *MNRAS*, 360, 974
 Hulse R. A., Taylor J. H., 1974, *ApJ*, 191, L59
 Hulse R. A., Taylor J. H., 1975a, *ApJ*, 201, L55
 Hulse R. A., Taylor J. H., 1975b, *ApJ*, 195, L51
 Lommen A. N., Zepka A., Backer D. C., McLaughlin M., Cordes J. M., Arzoumanian Z., Xilouris K., 2000, *ApJ*, 545, 1007
 Lorimer D. R., 2005, *Living Rev. Relativ.*, in press
 Lorimer D. R., Camilo F., Xilouris K. M., 2002, *ApJ*, 123, 1750
 Lorimer D. R. et al., 2004, *MNRAS*, 347, L21
 Lorimer D. R. et al., 2005, *MNRAS*, 359, 1524
 Lorimer D. R., Kramer M., 2005, *Handbook of Pulsar Astronomy*. Cambridge Univ. Press, Cambridge
 Lyne A. G. et al., 2004, *Sci*, 303, 1153
 Manchester R. N. et al., 2001, *MNRAS*, 328, 17
 McLaughlin M., Cordes J. M., Arzoumanian Z., 2000, in Kramer M., Wex N., Wielebinski N., eds, *ASP Conf. Ser. 202, IAU Colloq. 177, Pulsar Astronomy – 2000 and Beyond*. Astron. Soc. Pac., San Francisco, p. 41
 McLaughlin M. A., Arzoumanian Z., Cordes J. M., Backer D. C., Lommen A. N., Lorimer D. R., Zepka A. F., 2002, *ApJ*, 564, 333
 McLaughlin M. A. et al., 2004, in Camilo F., Gaensler B. M., eds, *Proc. IAU Symp. 218, Young Neutron Stars and their Environments*. Astron. Soc. Pac., San Francisco, p. 127
 McLaughlin M. A. et al., 2005, in Rasio F., Stairs I., eds, *Proc. Aspen Centre for Physics Conf. Binary Radio Pulsars*. In press
 Nice D. J., 1999, *ApJ*, 513, 927
 Nice D. J., Taylor J. H., 1995, *ApJ*, 441, 429
 Nice D. J., Fruchter A. S., Taylor J. H., 1995, *ApJ*, 449, 156
 Perillat P. J., 1999, 430 Linefeed Pointing After the Extension, Arecibo Technical Memo No. 99–11
 Qiao G. J., Lee K. J., Zhang B., Xu R. X., Wang H. G., 2004, *ApJ*, 616, L127
 Rankin J. M., 1983, *ApJ*, 274, 333
 Ray P. S. et al., 1995, *ApJ*, 443, 265
 Ray P. S., Thorsett S. E., Jenet F. A., van Kerkwijk M. H., Kulkarni S. R., Prince T. A., Sandhu J. S., Nice D. J., 1996, *ApJ*, 470, 1103
 Ruderman M. A., Sutherland P. G., 1975, *ApJ*, 196, 51
 Ruderman M., Shaham J., Tavani M., 1989, *ApJ*, 336, 507
 Shklovskii I. S., 1970, *Sov. Astron.*, 13, 562
 Stokes G. H., Segelstein D. J., Taylor J. H., Dewey R. J., 1986, *ApJ*, 311, 694
 Taylor J. H., Weisberg J. M., 1982, *ApJ*, 253, 908
 Thorsett S. E., Chakrabarty D., 1999, *ApJ*, 512, 288
 Toscano M., Sandhu J. S., Bailes M., Manchester R. N., Britton M. C., Kulkarni S. R., Anderson S. B., Stappers B. W., 1999, *MNRAS*, 307, 925
 Weisberg J. M., Taylor J. H., 1984, *Phys. Rev. Lett.*, 52, 1348
 Weltevrede P., Edwards R. T., Stappers B. W., 2005, *A&A*, in press (astro-ph/0507282)
 Wolszczan A. et al., 2000, *ApJ*, 528, 907
 Wolszczan A., Frail D. A., 1992, *Nat*, 355, 145
 York T., Jackson N., Browne I. W. A., Wucknitz O., Skelton J. E., 2005, *MNRAS*, 357, 124
 Zepka A., Cordes J. M., Wasserman I., Lundgren S. C., 1996, *ApJ*, 456, 305

This paper has been typeset from a $\text{\TeX}/\text{\LaTeX}$ file prepared by the author.